Strong broadband absorption in GaAs nanocone and nanowire arrays for solar cells

Baomin Wang, Erica Stevens, and Paul W. Leu*

Department of Industrial Engineering, University of Pittsburgh, Pittsburgh, PA 15261, USA

**pleu@pitt.edu*

http://lamp.pitt.edu

Abstract: We studied the influence of geometric parameters on the optical absorption of gallium arsenide (GaAs) nanocone and nanowire arrays via finite difference time domain simulations. We optimized the structural parameters of the nanocone and nanowire arrays to maximize the ultimate efficiency across a range of lengths from 100 to 1000 nm. Nanocone arrays were found to have improved solar absorption, short-circuit current density, and ultimate efficiencies over nanowire arrays for a wide range of lengths. Detailed simulations reveal that nanocones have superior absorption due to reduced reflection from their smaller tip and reduced transmission from their larger base. Breaking the vertical mirror symmetry of nanowires results in a broader absorption spectrum such that overall efficiencies are enhanced for nanocones. We also evaluated the electric field intensity, carrier generation and angle-dependent optical properties of nanocones and nanowires. The carrier generation in nanocone arrays occurs away from the surface and is more uniform over the entire structure, which should result in less recombination losses than in nanowire arrays.

OCIS codes: (040.5350) Photovoltaic; (350.6050) Solar energy; 310.6628 Subwavelength structures, nanostructures.

References and links

1. M. Green, "Limits on the open-circuit voltage and efficiency of silicon solar cells imposed by intrinsic auger processes," IEEE Trans. Electron. Devices **31**, 671–678 (1984).
2. M. D. Kelzenberg, S. W. Boettcher, J. A. Petykiewicz, D. B. Turner-Evans, M. C. Putnam, E. L. Warren, J. M. Spurgeon, R. M. Briggs, N. S. Lewis, and H. A. Atwater, "Enhanced absorption and carrier collection in Si wire arrays for photovoltaic applications," Nat. Mater. **9**, 239–244 (2010).
3. E. Garnett and P. Yang, "Light trapping in silicon nanowire solar cells," Nano Lett. **10**, 1082–1087 (2010).
4. K. Peng, Y. Xu, Y. Wu, Y. Yan, S. Lee, and J. Zhu, "Aligned single-crystalline Si nanowire arrays for photovoltaic applications," Small **1**, 1062–1067 (2005).
5. B. Wang and P. W. Leu, "Enhanced absorption in silicon nanocone arrays for photovoltaics," Nanotechnology **23**, 194003 (2012).
6. L. Hu and G. Chen, "Analysis of optical absorption in silicon nanowire arrays for photovoltaic applications," Nano Lett. **7**, 3249–3252 (2007).
7. C. Lin and M. L. Povinelli, "Optical absorption enhancement in silicon nanowire arrays with a large lattice constant for photovoltaic applications," Opt. Express **17**, 19371–19381 (2009).
8. B. Hua, B. Wang, M. Yu, P. W. Leu, and Z. Fan, "Rational geometrical design of multi-diameter nanopillars for efficient light harvesting," Nano Energy **2**, 951–957 (2013).

#201099 - $15.00 USD Received 11 Nov 2013; revised 16 Jan 2014; accepted 6 Feb 2014; published 18 Feb 2014

9. J. Caram, C. Sandoval, M. Tirado, D. Comedi, J. Czaban, D. A. Thompson, and R. R. LaPierre, "Electrical characteristics of core–shell p–n GaAs nanowire structures with te as the n-dopant," Nanotechnology **21**, 134007 (2010).
10. C. Colombo, M. Hei, M. Gratzel, and A. Fontcuberta i Morral, "Gallium arsenide p-i-n radial structures for photovoltaic applications," Appl. Phys. Lett. **94**, 173108 (2009).
11. G. E. Cirlin, A. D. Bouravleuv, I. P. Soshnikov, Y. B. Samsonenko, V. G. Dubrovskii, E. M. Arakcheeva, E. M. Tanklevskaya, and P. Werner, "Photovoltaic properties of p-doped GaAs nanowire arrays grown on n-type GaAs(111)B substrate," Nanoscale Res. Lett. **5**, 360–363 (2010).
12. J. A. Czaban, D. A. Thompson, and R. R. LaPierre, "GaAs Coreshell nanowires for photovoltaic applications," Nano Lett. **9**, 148–154 (2009).
13. C.-H. Sun, B. J. Ho, B. Jiang, and P. Jiang, "Biomimetic subwavelength antireflective gratings on GaAs," Opt. Lett. **33**, 2224–2226 (2008).
14. Y. M. Song, S. J. Jang, J. S. Yu, and Y. T. Lee, "Bioinspired parabola subwavelength structures for improved broadband antireflection," Small **6**, 984–987 (2010).
15. L. Wen, Z. Zhao, X. Li, Y. Shen, H. Guo, and Y. Wang, "Theoretical analysis and modeling of light trapping in high efficicency GaAs nanowire array solar cells," Appl. Phys. Lett. **99**, 143116 (2011).
16. H. Guo, L. Wen, X. Li, Z. Zhao, and Y. Wang, "Analysis of optical absorption in GaAs nanowire arrays," Nanoscale Res. Lett. **6**, 617 (2011).
17. N. Huang, C. Lin, and M. L. Povinelli, "Broadband absorption of semiconductor nanowire arrays for photovoltaic applications," J. Opt. **14**, 024004 (2012).
18. "Solar spectral irradiance: Air mass 1.5".
19. W. Shockley and H. J. Queisser, "Detailed balance limit of efficiency of p-n junction solar cells," J. Appl. Phys. **32**, 510–519 (1961).
20. E. D. Palik, *Handbook of Optical Constants of Solids* (Academic, 1997).
21. J. Berenger, "A perfectly matched layer for the absorption of electromagnetic waves," J. Comput. Phys. **114**, 185–200 (1994).
22. L. Cao, J. S. White, J. Park, J. A. Schuller, B. M. Clemens, and M. L. Brongersma, "Engineering light absorption in semiconductor nanowire devices," Nat. Mater. **8**, 643–647 (2009).
23. B. Wang and P. W. Leu, "Tunable and selective resonant absorption in vertical nanowires," Opt. Lett. **37**, 3756–3758 (2012).

1. Introduction

Light trapping is important for solar cells because it increases optical absorption in the photoactive region and allows for the achievement of high efficiencies with reduced material. Larger open circuit voltages and fill factors may be achieved by decreasing the amount of material since Auger recombination is decreased [1]. This is particularly important for GaAs solar cells, because gallium is a rare and expensive material and the processing costs associated with GaAs are high. Light trapping also relieves material purity and crystallinity requirements, since photogenerated minority carriers may diffuse shorter distances in order to be collected.

Light trapping structures such as vertical arrays of silicon nanowires and nanocones for the photoactive region have been studied extensively through experiments [2–4] and simulations [5–8]. GaAs nanowires [9–12] and nanocones [13, 14] have also been demonstrated experimentally. While there have been some simulation studies of GaAs nanowire arrays [15–17], there have yet to be any systematic studies of GaAs nanocones. In this paper, we report on detailed numerical investigations of the optical properties, short-circuit current densities, and solar conversion efficiencies of GaAs nanocone solar cells and compare their performance to that of GaAs nanowire solar cells and GaAs single pass thin films. We found that nanocone arrays exhibit enhancements over 20% compared to ideal single pass thin films for lengths $L \leq 300$ nm, and their performance always exceeds that of ideal single pass thin films. In contrast, nanowire arrays exhibit improvements over ideal single pass thin films only for lengths $L \leq 400$ nm. GaAs nanocones exhibit strong absorption over a broad portion of the solar spectrum above the band gap or broadband absorption due to reduced reflection from the small tip and reduced transmission from the broader base.

#201099 - $15.00 USD Received 11 Nov 2013; revised 16 Jan 2014; accepted 6 Feb 2014; published 18 Feb 2014

2. Method

Figure 1 shows the schematic of the GaAs nanocone arrays studied. The parameters of the structure are the length L of the nanocones, the period a of the square lattice, the top diameter d_{top}, and the bottom diameter d_{bot}. The top and bottom diameters of the nanocones are each smaller than or equal to the lattice period, $d_{top} \leq a$ and $d_{bot} \leq a$. GaAs nanowire arrays were also studied for comparison, which consist of nanocone arrays with the constraint $d_{top} = d_{bot} = d$ and $d \leq a$. We studied GaAs nanocones and nanowires for a wide variety of lengths from $L = 100$ to 1000 nm. GaAs is a direct band gap material with absorption lengths > 1 μm for photons with wavelength $\gtrsim 840$ nm ($E \lesssim 1.47$ eV). Thus, the lengths studied were smaller than 1000 nm, where light trapping may have significant benefit.

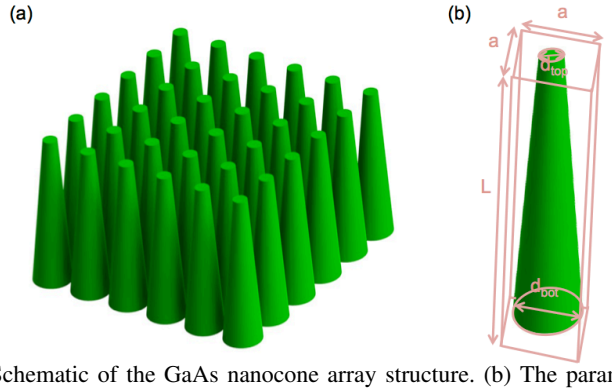

Fig. 1. (a) Schematic of the GaAs nanocone array structure. (b) The parameters for the array are the length L, the period a, the top diameter d_{top}, and the bottom diameter d_{bot}.

We employed the finite difference time domain (FDTD) method for solving Maxwell's equations. Time domain methods are well-suited for the computation of the energy dependent transmission $T(E)$, reflection $R(E)$, and absorption spectra $A(E)$. In order to evaluate the absorption performance of GaAs nanocone solar cells across the solar spectrum, we calculated the ultimate efficiency from

$$\eta = \frac{\int_{E_g}^{\infty} I(E)A(E)\frac{E_g}{E}dE}{\int_0^{\infty} I(E)dE} \tag{1}$$

where E is the photon energy, $E_g = 1.43$ eV is the band gap of GaAs, and $I(E)$ is the solar irradiance under the global 37° tilt Air Mass 1.5 spectrum [18]. The ultimate efficiency describes the efficiency of the cell when each photon absorbed produces one electron-hole pair, and these carriers are collected without recombination such as when the temperature of the cell is 0 K [19]. Assuming that each absorbed photon generates one electron-hole pair, and that all photogenerated carriers are collected, the short-circuit current density is

$$J_{sc} = q\int_{E_g}^{\infty} \frac{I(E)}{E}A(E)dE. \tag{2}$$

For each length L, we optimized the geometry for the greatest ultimate efficiency or equivalently, photocurrent generated for pitches a between 0 and 1500 nm with the constraints on d, d_{top}, and d_{bot} described above.

We evaluated the optical properties over the energy range of the solar spectrum from 0.62 to 4.4 eV (wavelengths from 2000 to 280 nm). We used the optical constants for GaAs obtained from experimental measurement results [20]. The experimental values from Palik [20] and the FDTD fitted values are shown in Fig. 2. While the fitted optical constants are close the

#201099 - $15.00 USD Received 11 Nov 2013; revised 16 Jan 2014; accepted 6 Feb 2014; published 18 Feb 2014

experimental values, the imaginary part k of the GaAs index of refraction below the band gap is small and does not drop sharply to 0 as seen in Fig. 2(b). Since the ultimate efficiency and short circuit current were calculated by only integrating over energies above E_g though, this numerical artifact does not affect the results in this paper. A uniform mesh of 20 nm $\times$ 20 nm $\times$ 20 nm was utilized where the ultimate efficiency was found to have converged within 1%. Perfectly matched layer boundary conditions were used for the upper and lower boundary of the simulation cell [21], and appropriate boundary conditions were used for the side boundaries to model the periodic nature of the arrays.

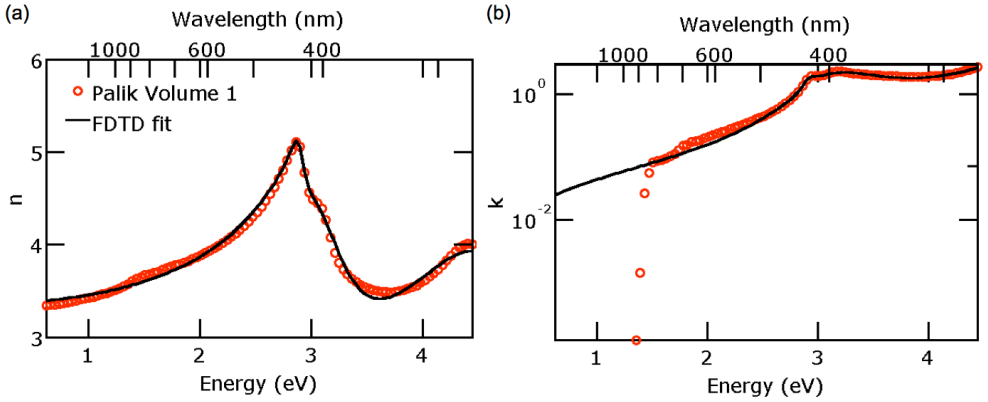

Fig. 2. Plots of the (a) real n and (b) imaginary part k of the GaAs refractive index. Values from Palik Volume 1 [20] and FDTD fitted values are shown.

3. Results and discussion

Figure 3(a) plots the optimal ultimate efficiency for GaAs nanocone, nanowire, and thin films as a function of active region length L. The GaAs thin films consist of a GaAs layer without any antireflection coatings. For reference, we also plot the ultimate efficiency of single pass thin films. The absorption for single pass thin films under normal incidence light is

$$A(E) = 1 - \exp[-\alpha(E)L] \tag{3}$$

where $\alpha(E)$ is the energy dependent absorption coefficient of GaAs. The single pass thin film assumes perfect antireflection where the light passes through the material only once with no light trapping. The short circuit current is shown on the right y-axis of Fig. 3(a). The short circuit current is linearly proportion to the ultimate efficiency under the assumption of perfect collection. Figure 3(b) plots the efficiency and short circuit current density enhancement of the nanowires and nanocones for each length compared to the single pass thin film. We found that while GaAs nanocones exhibit enhanced efficiencies and short circuit current densities over single pass thin films over all the lengths studied, GaAs nanowire arrays only have enhancements for lengths $L \leq 400$.

#201099 - $15.00 USD Received 11 Nov 2013; revised 16 Jan 2014; accepted 6 Feb 2014; published 18 Feb 2014

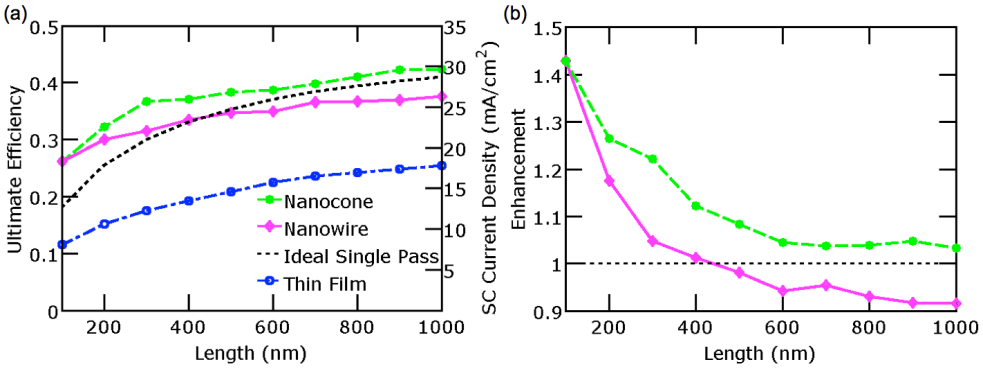

Fig. 3. (a) Optimal ultimate efficiency of GaAs nanowires and nanocones as compared with thin film and ideal single pass thin film. The short-circuit (SC) current density is shown on the right y-axis. (b) The ultimate efficiency enhancement from GaAs nanowires and nanocones compared to ideal single pass thin film.

Figures 4(a) and 4(b) plot the parameters for optimal nanowire and nanocone arrays at different lengths L respectively. For nanowire arrays, the optimal pitch varied between 500 nm and 700 nm, and the optimal diameter was between 400 and 600. These optimal parameters for vertical GaAs nanowire arrays are similar to those determined in Huang *et. al* for $L \leq 1000$ nm [17]. The volume filling factor (FF) of the nanowire arrays is $\frac{\pi d^2}{4a^2}$, and for the nanocone arrays $FF = \frac{\pi(d_{top}^2 + d_{top} * d_{bot} + d_{top}^2)}{4a^2}$. For nanocone structures, the optimal pitch was $a = 600$ nm for all lengths except when $L = 100$ nm. For $L = 100$ nm, the optimal nanocone array was the same as the nanowire array with $d_{top} = d_{bot} = d = 520$ nm. However, for lengths $L > 100$ nm, the optimal d_{top} was a small value between 200 nm and 400 nm and $d_{bot} = a$. This result will be discussed in more detail later in this paper.

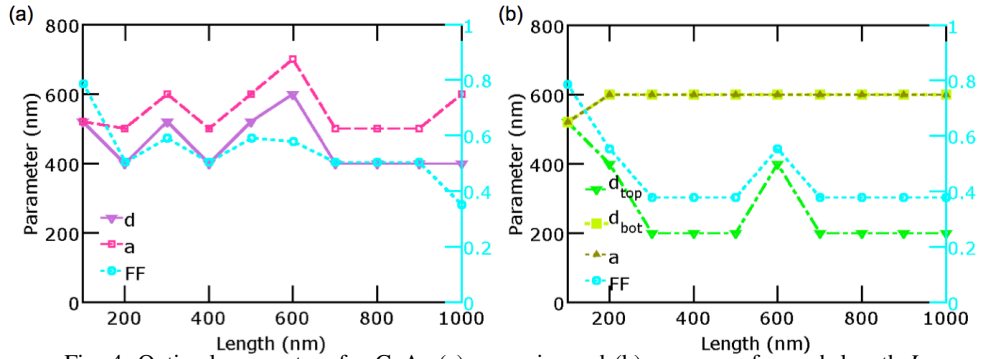

Fig. 4. Optimal parameters for GaAs (a) nanowire and (b) nanocone for each length L, respectively. The volume filling factor of the optimal structure is shown on the right y-axis of both plots.

We chose several representative nanowire and nanocone systems with $L = 300$ nm to compare their reflection, transmission, and absorption spectra. Figure 5 plots the (a) reflection $R(E)$, (b) transmission $T(E)$, and (c) absorption $A(E)$ spectra as a function of energy E for a small diameter nanowire array ($d = 200$ nm and $a = 600$ nm), the optimal nanowire array ($d = 520$ nm and $a = 600$ nm) , and the optimal nanocone array (d_{top} = 200 nm, d_{bot} = 600 nm, and a = 600 nm). The absorption was calculated by $A(E) = 1 - R(E) - T(E)$. The absorption of an ideal single pass thin film with $L = 300$ nm is also plot in Fig. 5(c) as calculated from Eq. (3). The reflection and transmission data shown for $E < E_g = 1.43$ eV were obtained through an

#201099 - $15.00 USD Received 11 Nov 2013; revised 16 Jan 2014; accepted 6 Feb 2014; published 18 Feb 2014

additional FDTD simulation, where the imaginary part of the GaAs refractive index was set to 0 to account for the numerical error in the FDTD fit shown in Fig. 2b. The ultimate efficiency for the single pass thin film is 30.0%. The optimal nanowire and nanocone arrays exhibit ultimate efficiencies of 31.4% and 36.6% respectively or enhancements of 4.7% and 22.0% respectively compared to that of the single pass thin film. The ultimate efficiency of the nanocone array is 16.5% higher than that of the nanowire array. The reflection, transmission, and absorption spectra of the nanowire system with $d = 200$ nm and $a = 600$ nm is also plotted, since this is the d_{top} of the optimal nanocone system.

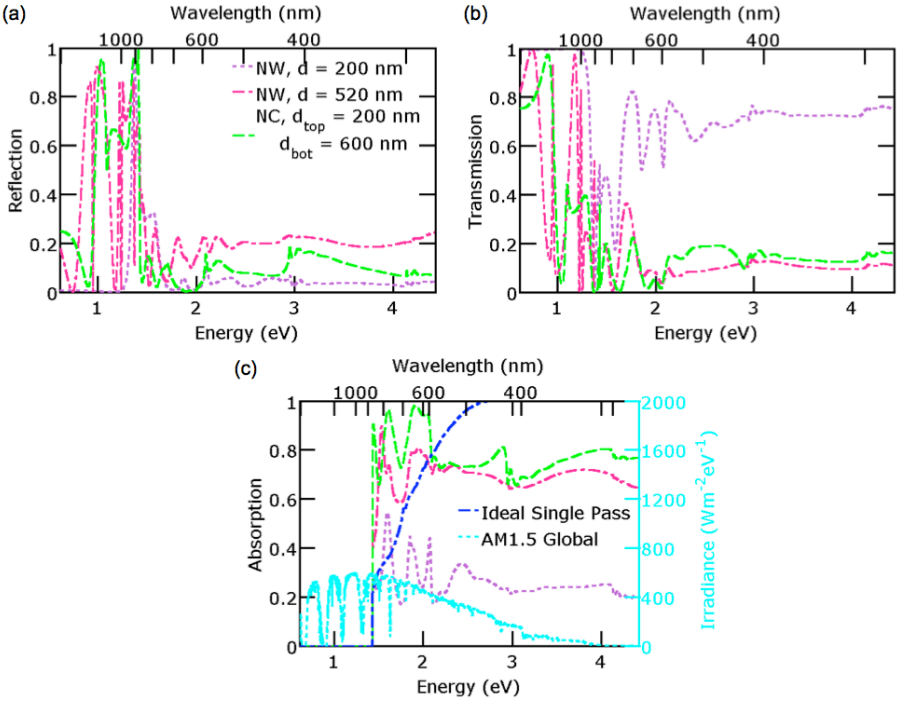

Fig. 5. Optical properties of three different GaAs nanostructures: nanowire (NW) arrays with $d = 200$ nm and $d = 520$ nm and nanocone (NC) arrays with $d_{top} = 200$ nm and $d_{bot} = 600$ nm. $a = 600nm$ in all three systems. (a), (b), and (c) show the reflectance, transmittance, and absorption spectra respectively. The absorption spectrum of the ideal single pass thin film is also plot in (c). The irradiance of the Air Mass 1.5 global solar spectrum is shown in right y-axis of (c).

Nanowire systems exhibit a tradeoff between reflection and transmission. Smaller diameter nanowire arrays such as the one illustrated with $d = 200$ nm have less reflection because there is less filling factor for light to reflect off the top of the nanowires. $FF = 0.09$ in these nanowire arrays. However, they also have higher transmission throughout the entire solar spectrum because there is less GaAs to absorb the light. Smaller diameter nanowires have better absorption in the infrared regime (< 1.67 eV), but poorer absorption in the ultraviolet regime (> 3.1 eV). On the other hand, larger diameter nanowire arrays, such as the optimal single diameter system with $d = 520$ nm exhibit higher reflection due to higher filling factor ($FF = 0.59$) and smaller transmission since there is more material to absorb the light. Larger diameter nanowire arrays have better absorption in the ultraviolet range, but slightly poorer absorption in the infrared range.

GaAs nanocone arrays address the tradeoff between reflection and transmission with a smaller d_{top} and a larger d_{bot}. The optimal GaAs nanocone array, with $d_{top} = 200$ nm and $d_{bot} =$

#201099 - $15.00 USD Received 11 Nov 2013; revised 16 Jan 2014; accepted 6 Feb 2014; published 18 Feb 2014

600 nm has reflection about the same of the small single diameter nanowire array with $d = 200$ nm, particularly in the visible and ultraviolet range. The larger base results in a transmission that is also low in the visible and ultraviolet regime. The GaAs nanocone array has absorption characteristics comparable to that of the best single diameter nanowire array in the ultraviolet range. However, in the visible and infrared range, the absorption is significantly improved. Table 1 lists the fraction of photons absorbed in different regions of the solar spectrum for these three representative nanowire and nanocone systems as well as the ideal single pass thin film. The ultraviolet region is from 3.1 to 4.4 eV (280 to 400 nm), the visible region is from 1.67 to 3.1 eV (400 to 740 nm), and the infrared region (above the GaAs band gap) is from 1.43 to 1.67 eV (740 to 867 nm). The total solar region shown only includes the range above the GaAs band gap energy from 1.43 to 4.4 eV (280 to 867 nm). The GaAs nanocone arrays have enhanced absorption compared to GaAs nanowire arrays over the entire spectral range due to anti-reflection and low transmission in the visible and ultraviolet ranges. Compared to the single pass thin film, the GaAs nanocones arrays have higher absorption except in the ultraviolet range.

Table 1. Absorption in different wavelength regimes. $a = 600$ nm in all three systems. The infrared and total solar regions are calculated for those portions that are above the GaAs band gap ($E > 1.43$ eV).

Spectrum Region	**NW d = 200 nm**	**NW d = 520 nm**	**NC, d_{top} = 200 nm d_{bot} = 600 nm**	**Single Pass**
Ultraviolet (%)	23	68	73	100
Visible (%)	27	71	81	77
Infrared (%)	35	67	83	32
Total Solar (%)	29	70	81	66

In order to understand the propagation of light in the nanowire and nanocone arrays, we simulated the electric field intensity $|\mathbf{E}(\mathbf{r},E)|^2$ and calculated the generation rate within the arrays from

$$G(\mathbf{r},E) = \frac{\varepsilon_i(E)\,|\mathbf{E}(\mathbf{r},E)|^2}{2\hbar} \tag{4}$$

where $\varepsilon_i(E)$ is the imaginary part of the dielectric constant, $\hbar$ is the reduced Planck constant, and $\mathbf{E}(\mathbf{r},E)$ is the position and energy-dependent electric field. By normalizing this quantity over the simulation power, and integrating over the solar spectrum energies as weighted by the solar irradiance $I(E)$, we obtained the solar-spectrum-weighted generation rate. Figure 6 shows the (a) solar-spectrum-weighted electric field intensity $|\mathbf{E}(\mathbf{r})|^2$ and (b) solar-spectrum-weighted generation rate $G(\mathbf{r})$ of the three representative nanowire and nanocone arrays for normal incident light integrated over photon energies $E = 1.43$ to 2.75 eV (or wavelengths $\lambda =$ 867 to 450 nm). This energy range encompasses about 83% of the power density available for absorption by GaAs. The contour plots show a cross-section through the center of the nanowire or nanocone. The electric field of the incoming electromagnetic wave was out of the plane of the paper in these simulations. The left column illustrates the optimal nanowire arrays with $d = 520$ nm, the middle column shows nanowire arrays with $d = 200$ nm, and the right column illustrates the optimal nanocone arrays with d_{top} = 200 nm and d_{bot} = 600 nm. $a = 600$ nm in all three systems. Dotted white lines indicate the edges of these GaAs nanostructures.

#201099 - $15.00 USD Received 11 Nov 2013; revised 16 Jan 2014; accepted 6 Feb 2014; published 18 Feb 2014

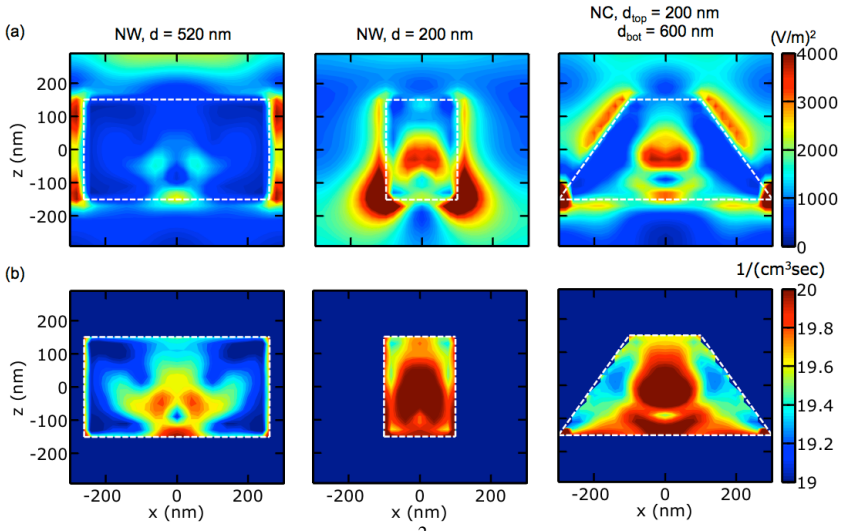

Fig. 6. The (a) electric field intensity $|\mathbf{E}(\mathbf{r})|^2$ and (b) solar-spectrum-weighted generation rate $G(\mathbf{r})$ for three representative GaAs nanowires and nanocones. From left to right, they are nanowire arrays with $d = 520$ nm, nanowire arrays with $d = 200$ nm, and nanocone arrays with d_{top} = 200 nm and d_{bot} = 600 nm. $a = 600$ nm in all three systems.

In the 200 nm diameter nanowire arrays, a large portion of the electromagnetic (EM) waves propagates outside the GaAs nanowire. The EM waves decay in the radial direction, such that a significant portion of the carrier generation is near the surface. While the reflection is low in these nanowire arrays due to their small diameter, the transmission is also higher since there is less GaAs to absorb the light, and the intensity of the electric field can be seen to be still significant near the bottom of the nanowire. In the 520 nm diameter nanowire arrays, most of the carrier generation occurs in the center of the nanowire away from the nanowire surface. There is more GaAs in the larger diameter nanowire arrays to absorb the EM waves, such that the electric field intensity is close to 0 at the bottom of the nanowire. However, because of the large filling factor or the large top of the nanowire, the reflection is substantial.

In the nanocone array, the EM field is seen to propagate further into structure. The small diameter d_{top} results in smaller reflection, while the larger base contains more GaAs to absorb the light. The electric field intensity is seen to decay to very small values near the bottom of the nanocone array, indicative of small transmission. The nanocone arrays have the advantage that the carrier generation occurs near the center of the nanocones, such that carriers are less likely to be affected by surface recombination. The carrier generation is still significant at the bottom of the nanocone. Furthermore, the carrier generation is more uniform along the length of the nanocone, such that photo-excited carriers are less likely to recombine, since the recombination rate is directly proportional to the local excess concentration of electrons and holes.

Guided resonance modes (also called leaky-mode resonances) have been shown to play a significant role in light absorption by nanowires [7, 22]. Nanowire arrays exhibit a mirror-symmetry plane about the mid-plane ($z = 0$), such that modes must be either symmetric or antisymmetric about the plane. Photonic crystal TE-like modes are odd with respect to z and TM-like modes are even with respect to z. Distinct peaks may be seen in the absorption spectrum of nanowire arrays corresponding to the coupling of incident light with these guided resonance modes. Guided resonance modes in horizontal nanowires [22] and vertical nanowires [23] may be tuned for the detection of particular energies or frequencies in photodetectors for example. In photovoltaics however, it is generally desirable for absorption to occur over a broad range of energies. By tapering the nanowires or forming nanocones, the mirror symmetry is

#201099 - $15.00 USD Received 11 Nov 2013; revised 16 Jan 2014; accepted 6 Feb 2014; published 18 Feb 2014

removed and the photonics crystal properties are lost. The absorption spectrum is broadened such that the overall absorption may be enhanced over that of nanowire arrays.

Finally, we simulated the angular dependence of the absorption spectrum of the optimal GaAs nanocone array as compared to the optimal nanowire array. Figure 7 plots the integrated absorption as a function of the zenith angle θ from 0 to 35 degrees for both TE and TM illumination. We found little variation in absorption with the azimuthal angle. The results show that for both transverse-electric (TE) polarization and transverse-magnetic (TM) polarization, the absorption of GaAs nanocone arrays and nanowire arrays increase a little bit and then decrease slightly, but that generally the absorption variation is small. The variation is about 5% for the nanocone array and about 8% for the nanowire array. In the low angle range (0 to 35 degrees), the absorption of both nanowire and nanocone arrays are not affected much by the angle of the incident light. With higher incidence angles, the difference in absorption between nanowires and nanocones become smaller as the vertical symmetry of nanowires is also broken at non-normal incidence angles. Nanocone arrays are slightly less sensitive than nanowire arrays to variation of incident light angle.

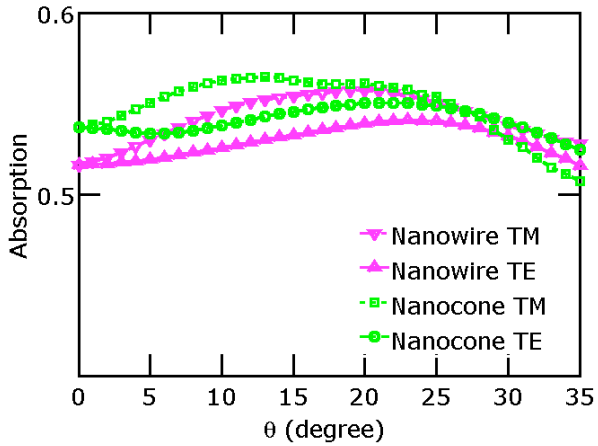

Fig. 7. Relationship between absorption and zenith angle θ of optimal nanowire and nancone arrays for TM and TE illumination.

4. Conclusion

In summary, we have studied the optical performances of GaAs nanocone arrays for photovoltaic application, and compared them with nanowire arrays for a variety of lengths. This novel structure can obtain enhanced absorption due to anti-reflection from the small tip and lower transmission due to the larger base. Nanocone arrays exhibit enhancements over 20% compared to ideal single pass thin films for lengths $L \leq 300$ nm, and their performance always exceeds that of ideal single pass thin films. Nanowire arrays also exhibit efficiency enhancements over ideal single pass thin films, but only for lengths $L \leq 400$ nm. Nanocone arrays have improved performance over nanowire arrays at all lengths except the shortest one studied where $L = 100$ nm. Nanocones may be fabricated by well-developed techniques, and are not particularly sensitive to specific geometry, which should facilitate their fabrication. We have also evaluated the solar-spectrum-weighted electric field intensity and generation rate in GaAs nanocone arrays and determined advantages of nanocone arrays over nanowire arrays in where carriers are photo-excited. Breaking the vertical mirror symmetry of nanowires results in broader absorption spectrum such that overall efficiencies may be enhanced. These efficiencies are also stable over a broad range of incident angles.

#201099 - $15.00 USD Received 11 Nov 2013; revised 16 Jan 2014; accepted 6 Feb 2014; published 18 Feb 2014

Acknowledgments

This work was supported in part by NSF grant #1233151. Computing resources were provided by the Center for Simulation and Modeling at the University of Pittsburgh. Erica Stevens would like to thank NSF NUE grant #1242075 and the Mascaro Center for Sustainable Innovation for support.

#201099 - $15.00 USD Received 11 Nov 2013; revised 16 Jan 2014; accepted 6 Feb 2014; published 18 Feb 2014